JOURNAL OF COMPUTATIONAL PHYSICS 117, 281–288 (1995)

Estimating Effective Properties of Composites from Cross-Sectional Photographs

JOHAN HELSING

NADA, Royal Institute of Technology, s-100 44 Stockholm, Sweden

Received May 13, 1994

An algorithm is presented for the rapid evaluation of certain functionals of three-point correlation functions, measured in a plane. This simplifies the estimation of effective physical properties of composite materials from cross-sectional photographs via bounds. More precisely, Fourier coefficients of a reduced three-point correlation function are expressed as inner products of polyharmonic fields. The polyharmonic fields are evaluated with a polyharmonic version of the fast multipole method with a CPU requirement proportional to the number p of fields included and to the number N of points in a discretization of the component interfaces. The Fourier coefficients are related to structural parameters which are used in third-order bounds on conductivity and elastic properties. Inclusion of p polyharmonic fields gives structural parameters with an error decaying at least as $1/p^3$. In a simple application for disks with $p = 10$, superalgebraic convergence in $1/N$, and a high-order Gaussian quadrature rule for the inner products, the algorithm gives an error of typically 0.05%. A previous algorithm, involving Monte Carlo integration, gives structural parameters with an error of typically 2%.

I. INTRODUCTION

How accurately can we estimate the effective physical properties of an isotropic three-dimensional composite, provided that we know the physical properties of the components but have only geometric information from cross-sectional photographs? A partial answer to this question has been known for a long time—it is in principle possible to find third-order bounds on effective properties, that is, upper and lower bounds that coincide to third order if they are expanded around homogeneity. In particular, for a two-component composite with component conductivities σ_1 and σ_2, and bulk and shear moduli κ_1, κ_2, μ_1, and μ_2 bounds on the effective properties σ_{eff}, κ_{eff}, and μ_{eff} can be found that coincide to third-order in $\sigma_2 - \sigma_1$, $\kappa_2 - \kappa_1$, and $\mu_2 - \mu_1$. These bounds involve two structural parameters denoted ζ_2 and η_2 which are functionals of a three-point correlation function Q_3 [1]. The function Q_3 can be measured from cross-sectional photographs.

Unfortunately, it has not yet been possible to measure Q_3 with an error less than about 1% and to evaluate ζ_2 and η_2 with an error less than about 2%. The reason for this being, among other things, the use of Monte Carlo techniques, for which the error decays as $1/\sqrt{M}$, where M is proportional to the size of the problem, for example, the number of discretization points used in an integral. See Berryman [2] for a discussion of these difficulties.

In this paper we present a radically different algorithm for the evaluation of ζ_2 and η_2 from cross-sectional photographs. We bypass the problem of estimating Q_3 and go directly for ζ_2 and η_2 using interface integral techniques involving polyharmonic Green's functions and the use of the fast multipole method [3]. As a result we get a method where the error decays with $1/M$ according to some high-order integration rule and as $1/p^3$ with the order p of the highest polyharmonic used. Numerical tests indicate that with $p = 10$ and extrapolation we may be able to evaluate structural parameters with an error less than 0.05%. Interface integral techniques have previously shown powerful for the evaluation of structural parameters and related quantities when full, that is three-dimensional, geometric information is available [4–10].

II. FOURIER EXPANSION OF PROBABILITY DENSITIES

With the use of variational techniques Milton [11] derived third-order bounds on σ_{eff}, κ_{eff}, and μ_{eff} for a three-dimensional composite that depend on volume fractions f_1 and f_2, on component properties σ_1, σ_2, κ_1, κ_2, μ_1, and μ_2, and on the two structural parameters

$$\zeta_2 = \frac{9}{2f_1f_2}\int_0^\infty\int_0^\infty\int_{-1}^1 \left(Q_3(r, s, \arccos u) - \frac{Q_2(r)Q_2(s)}{f_2}\right) \frac{P_2(u)}{rs}\,dudrds \tag{1}$$

and

$$\eta_2 = \frac{5\zeta_2}{21} + \frac{150}{7f_1f_2}\int_0^\infty\int_0^\infty\int_{-1}^1 \left(Q_3(r, s, \arccos u) - \frac{Q_2(r)Q_2(s)}{f_2}\right) \frac{P_4(u)}{rs}\,dudrds. \tag{2}$$

0021-9991/95 $6.00

In Eq. (1) and Eq. (2) $P_2(u)$ and $P_4(u)$ are the second and fourth Legendre polynomials, $Q_3(r, s, \theta)$ is the probability of a triangle, with two sides of length r and s at angle θ, having all three vertices lie in component two when placed randomly in the composite, and $Q_2(r)$ is the probability of a rod of length r having both vertices lie in component two when randomly placed in the composite.

Now introduce the reduced three-point probability density

$$R(\theta) = \int_0^\infty \int_0^\infty \left(Q_3(r, s, \theta) - \frac{Q_2(r)Q_2(s)}{f_2} \right) \frac{dr ds}{rs} \tag{3}$$

and its Fourier series coefficients

$$a_n = \frac{2}{\pi} \int_0^\pi R(\theta) \cos(2n\theta)\, d\theta, \quad n \geq 1. \tag{4}$$

Then substitution of variables and Fourier expansion in Eq. (1) and Eq. (2) gives the series

$$\zeta_2 = \frac{9}{8 f_1 f_2} \sum_{n=1}^{\infty} \left(\frac{1}{4n^2 - 1} - \frac{9}{4n^2 - 9} \right) a_n \tag{5}$$

and

$$\eta_2 = \frac{15}{32 f_1 f_2} \sum_{n=1}^{\infty} \left(\frac{-125}{4n^2 - 25} + \frac{27}{4n^2 - 9} + \frac{2}{4n^2 - 1} \right) a_n. \tag{6}$$

Since we expect $R(\theta)$ to be at least continuous and piecewise smooth, a_n will decay at least as fast as $1/n^2$ and the error in the series for ζ_2 and η_2, upon truncation after p terms, will decay at least as fast as $1/p^3$. On the other hand, should we know that $R(\theta)$ is continuous, but not smoother, we also know that the a_n decay, asymptotically, as $1/n^2$ and this can be used for extrapolation; if a_n are known up till $n = m$ we assume $a_{m+n} = a_m m^2/(m + n)^2$ and then sum Eq. (5) and Eq. (6) to infinity. The power of such an extrapolation is shown in Table I, where a_n is given, as calculated by Helte [12], and extrapolated and correct values for ζ_2 for a random aggregate of penetrable spheres at $f_2 = 0.7$. As can be seen, with $p = 10$, the error in ζ_2 is about 0.0004%.

TABLE I

The Fourier Coefficients a_n of Eq. (4) for a Random Aggregate of Penetrable Spheres at $f_2 = 0.7$, and Estimates for ζ_2 Based on the First p Coefficients a_p and Extrapolation

p	a_p	ζ_2^{extrap}	rel. err.
1	0.058684719	0.5589023	$4.5 \cdot 10^{-2}$
2	0.011447608	0.5834628	$2.8 \cdot 10^{-3}$
3	0.004554246	0.5847695	$5.4 \cdot 10^{-4}$
4	0.002411184	0.5849880	$1.7 \cdot 10^{-4}$
5	0.001485748	0.5850472	$6.9 \cdot 10^{-5}$
6	0.001005338	0.5850683	$3.3 \cdot 10^{-5}$
7	0.000724808	0.5850773	$1.8 \cdot 10^{-5}$
8	0.000547028	0.5850817	$1.0 \cdot 10^{-5}$
9	0.000427373	0.5850840	$6.3 \cdot 10^{-6}$
10	0.000343038	0.5850853	$4.1 \cdot 10^{-6}$

Note. The relative error decreases rapidly. The correct value for ζ_2 is 0.5850876995. See Ref. [12] for details on how a_p and ζ_2 were computed.

III. FOURIER COEFFICIENTS AS INNER PRODUCTS

In this section we will show how to express the Fourier coefficients a_n of Eqs. (4)–(6) as integrals over one of the components as seen on a cross-sectional photograph. We will do this by rewriting the triple integral γ_{2p}^* of Eq. (13) below in two different ways: By partial integration of Eq. (13) *with* the use of statistical averaging we arrive at Eq. (23) which contain the Fourier coefficients a_n. By partial integration of Eq. (13) *without* the use of statistical averaging we arrive at Eq. (26) which contains inner products of polyharmonic fields b_n, evaluated as integrals over component two. The formalism is a development of the results of Corson [13], Milton [11], Milton and Phan-Thien [14], and Helsing [9].

As a starting point consider a periodic composite in two dimensions. If the composite is a suspension component one denotes the matrix and component two denotes the inclusions. The unit cell is rectangular with volume V. Introduce $\Omega(\mathbf{r})$ as the indicator function for component two and divide it into a constant and a fluctuating part

$$\Omega(\mathbf{r}) = f_2 + \Omega'(\mathbf{r}) \tag{7}$$

The Fourier expansion of $\Omega(\mathbf{r})$ is

$$\Omega(\mathbf{r}) = f_2 + \sum_{\mathbf{k} \neq 0} \omega(\mathbf{k}) e^{i\mathbf{k}\cdot\mathbf{r}}, \tag{8}$$

where k runs over all reciprocal lattice points excluding the origin.

Define the auxiliary quantity

$$\gamma_{2p}^* = f_1 f_2^2 + \sum_{\mathbf{k} \neq 0} \sum_{\mathbf{m} \neq 0, \mathbf{k}} \frac{(\mathbf{k} \cdot \mathbf{m})^{2p}}{k^{2p} m^{2p}} \omega(-\mathbf{k}) \omega(\mathbf{k} - \mathbf{m}) \omega(\mathbf{m}) \tag{9}$$

and rewrite this

$$\gamma_{2p}^* = \sum_{\mathbf{k} \neq 0} \sum_{\mathbf{m} \neq 0} \sum_{\mathbf{n}} \frac{1}{V} \int_V \frac{(\mathbf{k} \cdot \mathbf{m})^{2p}}{k^{2p} m^{2p}} \omega(\mathbf{k}) \omega(\mathbf{m}) \omega(\mathbf{n}) e^{i(\mathbf{k}+\mathbf{m}+\mathbf{n})\cdot\mathbf{t}}\, dV_{\mathbf{t}}. \tag{10}$$

Periodicity and Green's second identity give

$$\frac{1}{k^{2p}} = \int_{V_\varepsilon} G_p(\mathbf{r}) e^{i(\mathbf{k}\cdot\mathbf{r})}\, dV_\mathbf{r}, \tag{11}$$

where V_ε is the unit cell excluding an infinitesimal disk around the origin, $\mathbf{r} = 0$, and $G_p(\mathbf{r})$ is the periodic Green's function for the polyharmonic operator

$$G_p(\mathbf{r}) = \sum_{i=1}^{\infty} - \left(\frac{|\mathbf{r} - \mathbf{r}_i|^2}{4}\right)^{p-1} \frac{\log |\mathbf{r} - \mathbf{r}_i|^2}{4\pi((p-1)!)^2}. \tag{12}$$

In Eq. (12) the lattice vector $\mathbf{r}_i$ runs over the entire plane. Equation (10) and Eq. (11) give

$$\gamma_{2p}^* = \frac{1}{V}\int_V \int_{V_\varepsilon} \int_{V_\varepsilon} G_p(\mathbf{r}) G_p(\mathbf{s}) \left\{\left(\frac{\partial}{\partial \mathbf{r}} \cdot \frac{\partial}{\partial \mathbf{s}}\right)^{2p} \Omega'(\mathbf{r}+\mathbf{t})\Omega'(\mathbf{s}+\mathbf{t})\Omega(\mathbf{t})\right\} dV_\mathbf{r} dV_\mathbf{s} dV_\mathbf{t}. \tag{13}$$

Repeated application of Gauss' theorem, integration over t, and the periodicity of $G_p(\mathbf{r})$ and $\Omega'(\mathbf{r})$ give

$$\gamma_{2p}^* = I_1 + I_2, \tag{14}$$

where

$$I_1 = \int_{S_\varepsilon}\int_{S_\varepsilon} \left\{\left(\frac{\partial}{\partial \mathbf{r}} \cdot \frac{\partial}{\partial \mathbf{s}}\right)^{2p-1} G_p^{\mathrm{fs}}(\mathbf{r}) G_p^{\mathrm{fs}}(\mathbf{s})\right\} (\mathbf{n}_\mathbf{r} \cdot \mathbf{n}_\mathbf{s}) \langle \Omega'(\mathbf{r})\Omega'(\mathbf{s})\Omega(\mathbf{0})\rangle\, dS_\mathbf{r} dS_\mathbf{s} \tag{15}$$

and

$$I_2 = \int_{V_\infty}\int_{V_\infty} \left\{\left(\frac{\partial}{\partial \mathbf{r}} \cdot \frac{\partial}{\partial \mathbf{s}}\right)^{2p} G_p(\mathbf{r}) G_p(\mathbf{s})\right\} \langle \Omega'(\mathbf{r})\Omega'(\mathbf{s})\Omega(\mathbf{0})\rangle\, dV_\mathbf{r} dV_\mathbf{s}, \tag{16}$$

where V_∞ denotes the entire space and angular brackets denote volume average. Recursion gives

$$\left(\frac{\partial}{\partial \mathbf{r}} \cdot \frac{\partial}{\partial \mathbf{s}}\right)^{2p-1} G_p^{\mathrm{fs}}(\mathbf{r}) G_p^{\mathrm{fs}}(\mathbf{s}) = \frac{(\mathbf{r}\cdot\mathbf{s})^{2p-1}}{4\pi^2 r^{2p} s^{2p}} \tag{17}$$

from which follows

$$\left(\frac{\partial}{\partial \mathbf{r}} \cdot \frac{\partial}{\partial \mathbf{s}}\right)^{2p} G_p^{\mathrm{fs}}(\mathbf{r}) G_p^{\mathrm{fs}}(\mathbf{s}) = \frac{p^2(\mathbf{r}\cdot\mathbf{s})^{2p}}{\pi^2 r^{2p+2} s^{2p+2}} - \frac{p(2p-1)(\mathbf{r}\cdot\mathbf{s})^{2p-2}}{2\pi^2 r^{2p} s^{2p}}. \tag{18}$$

The first integral on the right-hand side of Eq. (14) can be evaluated with Eq. (17) to

$$I_1 = \binom{2p}{p} \frac{f_1^2 f_2}{4^p}. \tag{19}$$

Rewrite the second integral on the right-hand side of Eq. (14) with Eq. (18) as

$$I_2 = \frac{2}{\pi 4^{p-1}} \sum_{n=0}^{p-1} (p-n)^2 \binom{2p}{n} \int_0^\infty \int_0^\infty \int_0^\pi \frac{\cos[2(p-n)\theta]}{rs} \langle \Omega(0)\Omega'(r)\Omega'(s,\theta)\rangle\, dr ds d\theta, \tag{20}$$

where the arguments (0), (r), and (s, θ) imply evaluation at the vertices of a triangle with two sides of length r and s and included angle θ. Then Eq. (7) can be used to show that for any two-component material

$$\langle \Omega(0)\Omega'(r)\Omega'(s,\theta)\rangle = Q_3(r, s, \theta) - f_2 Q_2(r) - f_2 Q_2(s) + f_2^3 \tag{21}$$

which gives with Eq. (4)

$$I_2 = \frac{1}{4^{p-1}} \sum_{n=0}^{p-1} (p-n)^2 \binom{2p}{n} a_{p-n}, \tag{22}$$

and from Eq. (14)

$$\gamma_{2p}^* = \frac{1}{4^p}\binom{2p}{p} f_1^2 f_2 + \frac{1}{4^{p-1}} \sum_{n=0}^{p-1} (p-n)^2 \binom{2p}{k} a_{p-n}. \tag{23}$$

Now rewrite Eq. (13) in a different way. Repeated application of Gauss' theorem gives

$$\gamma_{2p}^* = \frac{1}{V}\int_V \int_B \int_B \left\{\left(\frac{\partial}{\partial \mathbf{r}} \cdot \frac{\partial}{\partial \mathbf{s}}\right)^{2p-1} G_p(\mathbf{r}) G_p(\mathbf{s})\right\} (\mathbf{n}_\mathbf{r} dS_\mathbf{r} \cdot \mathbf{n}_\mathbf{s} dS_\mathbf{s}) \Omega(\mathbf{t})\, dV_\mathbf{t}, \tag{24}$$

where B is the interface between the components and $\mathbf{n}_\mathbf{s}$ and $\mathbf{n}_\mathbf{r}$ are normal vectors on B directed outwards from component two. Introduce the complex polyharmonic fields

$$\phi_p(t) = \sum_{i=1}^{\infty} \int_B \frac{(\bar{z} + \bar{z}_i - \bar{t})^{p-1} \cos\theta_z dS_z}{\pi(z + z_i - t)^p}, \tag{25}$$

where $\cos\theta_z$ is the angle between the outward normal on B and an arbitrarily chosen reference direction, and z_i are lattice vectors. With Eq. (17) we obtain

$$\gamma_{2p}^{*} = \frac{1}{4^p}\sum_{n=0}^{p-1}\binom{2p-1}{n} b_{p-n}, \tag{26}$$

where b_p is the integral over component two,

$$b_p = \frac{2}{V}\int_V \phi_p(z)\overline{\phi}_p(z)\Omega(z)\,dV_z. \tag{27}$$

The fields ϕ_p of Eq. (25) can be seen as caused by "polyharmonic charges" placed on the interface B.

In the next section we will show that, close to a point z_0, it is convenient to represent a polyharmonic field, such as ϕ_p of Eq. (25), on the form

$$\phi_p(z) = \sum_{n=0}^{p-1}\sum_{k=0}^{\infty} h_{nk}(\bar{z}-\bar{z}_0)^n(z-z_0)^k + \sum_{r=1}^{m}\frac{q_r(\bar{z}_r-\bar{z}+\bar{z}_0)^{p-1}}{(z_r-z+z_0)^p}, \tag{28}$$

where the first sum is a local expansion of the part of ϕ_p that originates from integrals over interfaces that are far away from z_0, and the second sum is a discretization of the contribution to ϕ_p from interfaces that are close to z_0. If ϕ_p of Eq. (25) is expressed as a local expansion only, the contribution to b_p of Eq. (27) can be evaluated as an interface integral

$$b_p^{\text{origin}} = \frac{2}{V}\sum_{n,m=0}^{p-1}\sum_{k,j=0}^{\infty} h_{nk}h_{mj}\int_{B_0}\operatorname{Re}\{z^{n+j}\hat{n}_z\}\operatorname{Re}\left\{\frac{z^{m+k+1}}{m+k+1}\right\}dS_z. \tag{29}$$

Identification of Eq. (23) and Eq. (26) gives the system of linear equations

$$\binom{2p}{p}f_1^2 f_2 + 4\sum_{n=1}^{p} n^2\binom{2p}{p-n}a_n = \sum_{n=1}^{p}\binom{2p-1}{p-n}b_n, \tag{30}$$

from which the Fourier coefficients a_n can be expressed in the inner products b_m of order $m \le n$.

IV. FAST EVALUATION OF POLYHARMONIC FIELDS

In this section we will present the tools necessary to evaluate the polyharmonic interface integrals ϕ_p of Eq. (25) with the fast multipole method. The treatment follows Greenbaum, Greengard, and Mayo [15] for a biharmonic field. We therefore only state results.

Suppose that m points z_i are located within a disk of radius R centered at the origin. Then, for a point z with $|z| > R$, the field

$$\phi_p(z) = \sum_{i=1}^{m}\frac{q_i(\bar{z}_i-\bar{z})^{p-1}}{(z_i-z)^p} \tag{31}$$

can be represented by a polyharmonic expansion of the form

$$\phi_p(z) = \sum_{n=0}^{p-1}\sum_{k=p}^{\infty}\frac{(k-1)!A_{k-p}^{p-n-1}\bar{z}^n}{n!z^k}, \tag{32}$$

where

$$A_s^r = \sum_{i=1}^{m}\frac{-q_i(-\bar{z}_i)^r z_i^s}{r!s!}. \tag{33}$$

Translation of a far field expansion: Suppose that

$$\phi_p(z) = \sum_{n=0}^{p-1}\sum_{k=p}^{\infty}\frac{(k-1)!A_{k-p}^{p-n-1}(\bar{z}-\bar{z}_0)^n}{n!(z-z_0)^k}, \tag{34}$$

is a far field expansion of Eq. (31) due to a set of m sources of strengths $q_1, q_2, \ldots, q_m$, all of which are located inside the circle D of radius R with center at z_0. Then for z outside the circle D_1 of radius $R + |z_0|$ and center at the origin,

$$\phi_p(z) = \sum_{n=0}^{p-1}\sum_{k=p}^{\infty}\frac{(k-1)!B_{k-p}^{p-n-1}\bar{z}^n}{n!z^k}, \tag{35}$$

where

$$B_s^r = \sum_{i=0}^{r}\sum_{j=0}^{s}\frac{A_{s-j}^{r-i}(-\bar{z}_0)^i z_0^j}{i!j!}. \tag{36}$$

Conversion of a far field expansion into a local expansion: Suppose that Eq. (31) is the polyharmonic field from charges at the points $z_1, z_2, \ldots, z_m$ all of which are located inside the circle D_1 with radius R and center at z_0 and that $|z_0| > (c+1)R$ with $c > 1$. Then the corresponding far field expansion of Eq. (34), truncated at order w, converges inside the circle D_2 of radius R centered about the origin. Inside D_2 the truncated far field expansion is described by the power series

$$\phi_p(z) = (-1)^p\sum_{n=0}^{p-1}\sum_{k=0}^{w-n}\frac{C_{p+k}^{p-n-1}\bar{z}^n z^k}{n!k!}, \tag{37}$$

where

$$C_s^r = \sum_{i=0}^{r}\sum_{j=0}^{w}\frac{(-1)^j(s+j-1)!A^{r-i}(-\bar{z}_0)^i}{i!z_0^{s+j}}. \tag{38}$$

Translation of a local expansion: Suppose that

$$\phi_p(z) = (-1)^p \sum_{n=0}^{p-1} \sum_{k=0}^{w-n} \frac{C_{p+k}^{p-n-1}(\bar{z} - \bar{z}_0)^n (z - z_0)^k}{n!k!}. \tag{39}$$

Then

$$\phi_p(z) = (-1)^p \sum_{n=0}^{p-1} \sum_{k=0}^{w-n} \frac{D_{n+k+1}^{p-n-1} \bar{z}^n z^k}{n!k!}, \tag{40}$$

where

$$D_s^r = \sum_{i=0}^{r} \sum_{j=0}^{w-s} \frac{C_{r+s+j}^{r-i}(-\bar{z}_0)^j (-z_0)^j}{i!j!}. \tag{41}$$

The preceding results enable the implementation of the fast multipole method fully analogous to the description in Greenbaum, Greengard, and Mayo [15]. Furthermore, it follows from our particular choice of indexation that for series of fields ϕ_p, where the charges q_i and positions z_i of Eq. (31) are independent of p, the coefficients A_s^r, B_s^r, C_s^r, and D_s^r will be independent of p as well. This means that fields ϕ_p of different orders p can be evaluated simultaneously with a reduction in the computational cost. More precisely, the work of evaluating p fields ϕ_p becomes proportional to p, rather than to p^2, which holds if this simplification is not utilized. Clearly, the series of fields ϕ_p which result from discretization of Eq. (25) are of this type.

V. NUMERICAL EXAMPLE FOR DISKS

The fast multipole method in two dimensions has been implemented by various research groups in different varieties. For example, there are implementations for both free-space and periodic evaluations suitable for uniform distributions of harmonic charges [3] and there is a so-called adaptive code suitable for evaluations when harmonic charges are not uniformly distributed [16]. For uniformly distributed biharmonic charges there is a free-space code [15].

The evaluation of ϕ_p of Eq. (25) for general photographs with the method of the previous section requires an adaptive polyharmonic fast multipole code. Adaptivity is needed, since the charges will be lined up on the component interfaces, and not uniformly distributed in the plane. The programming of such an adaptive polyharmonic code, however straightforward, is quite a demanding task. As a numerical example and as a check on the algorithms presented I will here treat a model for which simplifications in the programming can be made: a cross sectional photograph that looks like a square array of disks, with unit cell of unit length, where the disks have radii R and occupy a volume fraction f_2 and where one disk is centered at the origin. Note that this model is somewhat artificial, since it does not correspond to the photograph of a composite that is statistically isotropic.

The field ϕ_p of Eq. (25) at the disk at the origin can be represented on the form of Eq. (28) in two different ways; the contribution from *all* disks in the plane can be treated as a far field represented by a local expansion, or the contribution from those eight disks that are nearest neighbours to the disk at the origin can be treated with direct interaction through discretization of the integral of Eq. (25), a near field, while the contribution from all other disks is treated as a far field represented by a local expansion. Should we choose to distinguish between far field and near field in this way we may place m discretization points z_r, according to the trapezoidal quadrature rule, on each of the eight nearest neighbour disks. This gives for z inside the disk at the origin

$$\begin{aligned}\phi_p(z) = \delta_{p1} &+ \sum_{n=0}^{p-1} \sum_{k=0}^{w} \frac{E_{p+k}^{p-n}(-\bar{z})^n z^k}{n!k!} \\ &+ \sum_{r=m+1}^{9m} \frac{2R\cos\theta_r}{m} \frac{(\bar{z}_r - \bar{z})^{p-1}}{(z_r - z)^p},\end{aligned} \tag{42}$$

where δ_{jk} is the Kronecker symbol,

$$\begin{aligned}E_s^r = &\sum_{i=0}^{r-1} \left(\frac{f_2}{\pi}\right)^{i+1} \frac{(-1)^{i+1}(s+i)! S_{r+s}^{r-i}}{i!(r-i-1)!(i+1)!} \\ &- \sum_{i=1}^{r-1} \left(\frac{f_2}{\pi}\right)^{i} \frac{(-1)^i (s+i-2)! S_{r+s-2}^{r-i}}{i!(r-i-1)!(i-1)!},\end{aligned} \tag{43}$$

θ_r is the angle between the real axis, used as reference direction, and the interface normal direction at z_r and

$$S_n^p = \sum_{s=10}^{\infty} \frac{\bar{z}_s^{p-1}}{z_s^{n-p+1}} \tag{44}$$

are lattice sums; the lattice vector z_s runs over all lattice points in the plane, excluding the origin and its eight nearest neighbours. (Should we choose to represent ϕ_p of Eq. (42) as a far field only, the eight nearest neighbours should be included in the lattice sum, as well.) The series of lattice sums S_n^1 was introduced in composite literature by Rayleigh [17]. The series S_n^2 has previously been used by myself for elasticity calculations [9].

Should we choose to represent ϕ_p of Eq. (42) as a far field only Eq. (29) with $p = 1$ gives

$$\begin{aligned}b_1 = 2 &\\ &\left(f_1^2 f_2 + f_2 \sum_{k=1}^{w} (4k-1)\left(4 + \frac{(-1)^k}{4^{k-1}} + S_{4k}^1\right)^2 \left(\frac{f_2}{\pi}\right)^{4k}\right)\end{aligned} \tag{45}$$

and with $p \geq 2$

$$b_p = 2f_2 \sum_{n,q=0}^{p-1} \sum_{k,j=0}^{w} \frac{E_{p+k}^{p-n} E_{p+j}^{p-q} (f_2/\pi)^{k+q} (-1)^{q+n} \delta_{j(k+q-n)}}{n!k!q!j!(k+q+1)}. \tag{46}$$

TABLE II

Numerical Values of the First Nonvanishing Lattice Sums S^g_{2p+2} of Eq. (44)

S^1_4	3.15121200215390
S^3_8	5.03066621465737
S^5_{12}	3.44188692377912
S^7_{16}	5.4947062432777
S^9_{20}	3.0302835730502

Note. The calculations are made with a simplified version of the fast multipole method, and the first eight digits of each sum is checked with direct summation. For a discussion of fast algorithms for lattice sum evaluation, see Ref. [19].

For the evaluation of Eq. (46), as well as for the implementation of a general periodic polyharmonic fast multipole code, p of the series of lattice sums S^p_n with $n \geq 2p$ must be computed. For $n \geq 2p + 4$ these sums are easily computed by direct summation. For $n = 2p + 2$, and if the sum does not vanish, the convergence of the direct summation will be very slow. In Table II we present the first five nonvanishing sums S^g_{2p+2} calculated with a polyharmonic analogue to the simplified fast multipole method used previously [7]. In short, this algorithm computes the far field expansion outside supercells including an exponentially growing number of charges. This is done by recursion of Eq. (39) and Eq. (40). The contribution to the lattice sums from various far fields is computed with Eq. (37) and Eq. (38).

For $n = 2p$ the lattice sums of Eq. (46) are only conditionally convergent and we assign the physically relevant values to them by demanding periodicity of the field that results from unit polyharmonic charges $\bar{z}^{p-1}/z^p$ placed at every lattice point [3]. Equating the fields at, for example, $z = \frac{1}{2}$ and $z = -\frac{1}{2}$ gives

$$\sum_{r=1}^{\infty} \frac{(\bar{z}_r - 0.5)^{p-1}}{(z_r - 0.5)^p} = \sum_{r=1}^{\infty} \frac{(\bar{z}_r + 0.5)^{p-1}}{(z_r + 0.5)^p}, \tag{47}$$

and by series expansion

TABLE III

Numerical Values of the First 10 Conditionally Convergent Lattice Sums S^g_p of Eq. (44), Computed According to Eq. (48)

S^1_2	$3.1415926535898K$
S^2_4	2.0784511611614
S^3_6	$1.0471975511966K$
S^4_8	0.7903136267083
S^5_{10}	$0.62831853071795K$
S^6_{12}	2.3581519979779
S^7_{14}	$0.44879895066288K$
S^8_{16}	2.9191682611277
S^9_{18}	$0.34906585051680K$
S^{10}_{20}	0.8271159154874

Note. K is a conjugating operator. The numerical values for S^1_2 and S^2_4 coincide, to the last digit, with results of Ref. [9].

TABLE IV

Numerical Values of the First 10 Numbers γ^*_{2p} for a Square Array of Disks at $f_2 = 0.7$

	Eq. (9)	Eq. (26)
γ^*_2	0.057474	0.057470732425347
γ^*_4	0.058993	0.058990471293056
γ^*_6	0.060257	0.060254670947156
γ^*_8	0.061064	0.061062899186933
γ^*_{10}	0.061616	0.061615676270128
γ^*_{12}	0.062053	0.062053566530432
γ^*_{14}	0.062449	0.062450404733132
γ^*_{16}	0.062839	0.062839944694868
γ^*_{18}	0.063233	0.063235068725672
γ^*_{20}	0.063637	0.063638686495525

Note. The left column comes from Eq. (9) using $k, m \leq 200$ and linear extrapolation. The right column is Eq. (26) with Eq. (46).

$$\tilde{S}^g_{2p} = \frac{4}{p} + \frac{1}{p}\sum_{j=1}^{p-1}\sum_{n=p}^{\infty}\binom{p-1}{j-1}\binom{n-1}{p-1}\frac{(-1)^{p+n}\tilde{S}^j_{n+j-1}}{2^{n-j-1}} - \frac{1}{p}\sum_{n=1}^{\infty}\binom{p+2n}{2n+1}\frac{\tilde{S}^g_{2p+2n}}{4^n}, \tag{48}$$

where the tilde over S means that a contribution from nearest neighbour lattice points are included in the sum. Equating the fields at $z = i/2$ and $z = -i/2$ gives an expression similar to Eq. (48), but which differs in terms of signs. To resolve this inconsistency we propose that for odd p a conjugating operator K should be attached to the sum S^g_{2p}. When this is done the sums of Eq. (48) become independent of the choice of the pair of points for field evaluation. Furthermore, it has been shown previously that for calculations on disks the sum S^1_2 should indeed include a conjugating operator [7]. The 10 first sums S^g_{2p}, without contributions from nearest neighbours, are presented in Table III.

When the field ϕ_p of Eq. (42) is represented by a far field only, the evaluation of the sums for b_n of Eq. (46) is quick, but many terms in the local expansion are needed which will eventually limit the accuracy for large p due to cancellations. As a check on most of the expressions derived so far, I computed the quantities γ^*_{2p} in two independent ways, first according to Eq. (26) with Eq. (46), far field only, and local expansions up to order 80 aiming at full accuracy—then according to Eq. (9) using $k, m \leq 200$ and linear extrapolation aiming at four-digit accuracy. Results for $f_2 = 0.7$ are presented in Table IV. For b_p up to $p = 10$ and the first method of computation typically required 10 s on a workstation while the second method required several days. In Table V we present the coefficients b_n and a_n computed via Eq. (46) and Eq. (30) and extrapolated values for ζ_2.

If the field ϕ_p of Eq. (42) is represented by a sum of a far field and a near field computed with direct summation, the local

expansion of the far field at the origin will converge quicker than if ϕ_p is represented by a far field only. Fewer terms in the local expansions are needed for a prescribed accuracy. But if too many discretization points are included in the the near field zone, much time will be spent on summation and the evaluation f b_p of Eq. (27) with Eq. (28) becomes slow. In Table 5 we also give b_p for the square array of disks at $f_2 = 0.7$ computed with 40 terms in the local expansion and 400 equispaced discretization points on each of the eight disks that are nearest neighbours to the disk at the origin. The general purpose NAG subroutine D01DAF, based on a family of Gaussian quadrature rules, was used for b_p with between 3000 and 12,000 integrand evaluations per integral. These computations took from 2 to 8 min per integral on a workstation.

VI. FURTHER IMPROVEMENT FOR THE CONDUCTIVITY

Once the structural parameter ζ_2 of Eq. (5) has been computed, third-order lower and upper bounds on the effective conductivity of the composite can be evaluated according to

$$\sigma_{\text{eff}}^{\text{low}} = \sigma_1 \frac{(\sigma_1 + 2\sigma_2)(\sigma_2 + 2(f_1\sigma_1 + f_2\sigma_2)) - 2f_1\zeta_2(\sigma_2 - \sigma_1)^2}{(\sigma_1 + 2\sigma_2)(2\sigma_1 + (f_1\sigma_2 + f_2\sigma_1)) - 2f_1\zeta_2(\sigma_2 - \sigma_1)^2} \tag{49}$$

and

$$\sigma_{\text{eff}}^{\text{up}} = (f_1\sigma_1 + f_2\sigma_2) - \frac{f_1 f_2(\sigma_2 - \sigma_1)^2}{3\sigma_1 + (f_1 + 2\zeta_2)(\sigma_2 - \sigma_1)}, \tag{50}$$

where in Eq. (49) $\sigma_1 \leq \sigma_2$ is assumed [1, 18]. For small ratios $(\sigma_2 - \sigma_1)/(\sigma_2 + \sigma_1)$ these bounds are tight and give a useful estimate. If the conductivities of the two components differ more, the bounds are not so informative. Then, to get a possibly improved lower bound, we may proceed to calculate the effective conductivity of the cross-sectional photograph as if it were a so-called fiber reinforced material, that is, translationally invariant in the direction perpendicular to the cross-sectional surface. Clearly, if one of the component forms a connected path across the photograph, and if this component has high enough conductivity, the transverse effective conductivity of the cross-sectional surface will be a better lower bound than Eq. (49).

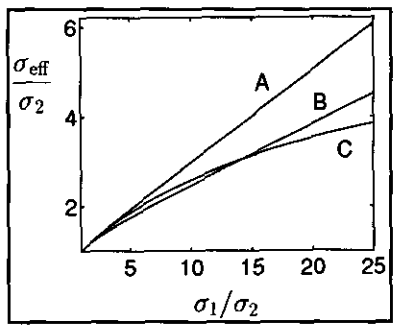

FIG. 1. Bounds on the effective conductivity of an assumed isotropic composite from cross-sectional information. Curves A and C are the upper and lower third-order bounds of Eq. (49) and Eq. (50) with ζ_2 computed with the method of this paper. Curve B is the effective conductivity computed with Rayleigh's method as if the composite was translationally invariant and constitutes a lower bound. A square array of disks with disk area fraction $f_2 = 0.7$ is used as photograph.

Accurate calculations of the effective conductivity of two-dimensional suspensions with inclusions that do not lie too close to each other have recently been performed by Greengard and Moura [6]. They used an integral equation method that was accelerated with iterative techniques and the fast multipole method. Rayleigh's method [17], which is easy to implement but works for suspensions of disks and spheres only, can also be accelerated in a similar manner [7]. We computed the effective conductivity for the square array of disks at $f_2 = 0.7$ when the disks have unit conductivity, $\sigma_2 = 1$, and the surrounding matrix has a conductivity σ_1 that varies from unity to 25. This was done with Rayleigh's method. Comparison with the bounds of Eq. (49) and Eq. (50) with ζ_2 from Eq. (5) is shown in Fig. 1. We see that in our example this computation gives an improvement over the bound of Eq. (49) for $\sigma_1/\sigma_2 \gtrsim 14$.

VII. DISCUSSION

We have presented a new algorithm to evaluate structural parameters of statistically isotropic composites from cross-sectional photographs. In particular we discussed the structural parameters ζ_2 and η_2 which enter into third-order bounds on the conductivity and elastic moduli of two-component compos-

TABLE V

Interface Integrals b_p of Eq. (27) and Fourier Coefficients a_p of Eq. (4) and Eq. (30) for a Square Array of Disks at $f_2 = 0.7$

p	b_p^1	b_p^2	a_p	ζ_2^{extrap}
1	0.22988292970139		0.02597073242535	0.24734
2	0.25419875158474	0.25419875	0.009394738867709	0.22523
3	0.28647588568042	0.28647589	0.003782223994363	0.22619
4	0.24269466926405	0.24269467	0.001664603210422	0.22686
5	0.27912431724715	0.27912431	0.001725897117801	0.22618
6	0.3928115271342	0.39281153	0.001529318162182	0.22592
7	0.435350221458	0.43535022	0.0010975939087	0.22594
8	0.37487495071	0.37487495	0.000624009940	0.22606
9	0.3541217952	0.35412180	0.000599923613	0.22600
10	0.403978968	0.40397897	0.00052400929	0.22599

Note. The b_p^1 are computed with ϕ_p of Eq. (25) represented as a far field only. Local expansions of order 80 were used. The b_p^2 are computed with ϕ_p represented with a sum of a far field and a near field as in Eq. (42). Four hundred discretization points per disk and local expansions of order 40 were used. The extrapolated estimates for ζ_2 of Eq. (5) are based on the pth coefficient a_p and on the assumption that a_p decay like $1/p^2$.

ites [1], but the algorithm also applies to the evaluation of structural parameters for multicomponent composites.

A previous algorithm [2] first estimates a three-point correlation function $Q(r, s, \theta)$ by direct measurement in a photograph, and then computes ζ_2 and η_2 by indefinite three-dimensional Monte Carlo integration in Eq. (1) and Eq. (2). The error in this algorithm decays as $1/\sqrt{M}$, where M is the number of discretization points and a typical accuracy is 2%. Our algorithm discretizes the component interfaces, as seen on the photograph. Polyharmonic fields, ϕ_n, are evaluated with a polyharmonic version of the fast multipole method. Fourier coefficients, a_n, related to Q_3, are computed via inner products, b_n, of the ϕ_n over one of the components. The work for the evaluation of all the ϕ_n is proportional to pN, where p is the index of the highest ϕ_n used and N is the number of discretization points on the component interfaces. The work for the evaluation of the two-dimensional integrals b_n may depend on the shape of the boundary interfaces. But, in principle, by subdividing the region of integration into subregions, one should always be able to evaluate b_n with some high-order integration rule. Finally, the parameters ζ_2 and η_2 are expressed as a sum over the a_n. Upon truncation of these sums after p terms the error in ζ_2 and η_2 decays at least as fast as $1/p^3$.

We discussed two numerical examples. First the random aggregate of permeable spheres, for which the three-point correlation functions Q_3, structural parameters ζ_2 and η_2, and Fourier coefficients a_p can be computed accurately with another method than that of this paper [12]. We observed, see Table I, that a_p decayed smoothly as $1/p^2$. This, in turn, could be used for very accurate extrapolation; 10 coefficients a_n gave ζ_2 with an error of only 0.0004%. Then we considered a photograph that looks like a square array of disks. This example is somewhat artificial since it does not correspond to a cross-sectional photograph of a statistically isotropic three-dimensional composite, but it has the advantage that it can be solved with only a moderate programming effort. As can be seen in Table V the coefficients a_p decay as $1/p^2$, but not at all as smoothly as in Table I. Consequently, the error in the extrapolated ζ_2 may be of the order 0.05%. It is tempting to believe that a smooth $1/p^2$ decay of a_p is the typical behaviour for a statistically isotropic material. If so, the accuracy of our algorithm may be much better than claimed in the introduction.

ACKNOWLEDGMENTS

This work was supported by TFR Grant 92-961 to Anders Szepessy and a TFR Grant to the Center for Computational Mathematics and Mechanics C ^{2}M^2.

REFERENCES

1. G. W. Milton, *Phys. Rev. Lett.* **46,** 542 (1981)
2. J. G. Berryman, *J. Comput. Phys.* **75,** 86 (1988).
3. L. Greengard and V. Rokhlin, *J. Comput. Phys.* **73,** 325 (1987).
4. G. W. Milton, R. C. McPhedran, and D. R. McKenzie, *Appl. Phys.* **25,** 23 (1981).
5. J. Hetherington and M. F. Thorpe, *Proc. R. Soc. London A* **438,** 591 (1992).
6. L. Greengard and M. Moura, *Acta Numerica,* (Cambridge University Press: Cambridge, 1994) pp. 379–410.
7. J. Helsing, *Proc. R. Soc. London A,* **445,** 127–140 (1994).
8. J. Helsing, *J. Math. Phys.* **35,** 1688 (1994).
9. J. Helsing, *J. Mech. Phys. Solids,* **42,** 1123–1138 (1994).
10. L. Greengard and J. Helsing, *J. Appl. Phys.,* in press.
11. G. W. Milton, *J. Mech. Phys. Solids* **30,** 177 (1982).
12. A. Helte, in preparation.
13. P. B. Corson, *J. Appl. Phys.* **45,** 3171 (1974).
14. G. W. Milton and N. Phan-Thien, *Proc. R. Soc. London A* **380,** 305 (1982).
15. A. Greenbaum, L. Greengard, and A. Mayo, *Physica D* **60,** 216 (1992).
16. J. Carrier, L. Greengard, and V. Rokhlin, *SIAM J. Sci. Stat. Comput.* **9,** 669 (1988).
17. J. W. Rayleigh, *Phil. Mag.* **34,** 481 (1892).
18. G. W. Milton, in *Physics and chemistry of porous media,* edited by D. L. Johnson and P. N. Sen (Amer. Inst. of Phys., New York, 1984), p. 66.
19. L. Berman and L. Greengard, *J. Math. Phys.* **35,** 6036 (1994).